Food & Function

ROYAL SOCIETY OF CHEMISTRY

PAPER

View Article Online
View Journal | View Issue

Cite this: *Food Funct.*, 2025, **16**, 2824

Dietary alpha-lipoic acid alleviates heat stress by modulating insulin-like signaling to maintain homeostasis *in C. elegans*

Longnong You,†[a,b] Zirui Huang,†[a,b] Wenyuan He,[b] Lizhu Zhang,[b] Haiyang Yu,[b] Yaoyong Zeng,[b] Yan Huang,[c] Shaoxiao Zeng*[a] and Lingjun Zheng *[b]

Prolonged exposure to high temperatures can cause oxidative stress in the body, negatively impacting human health. Alpha-lipoic acid (ALA) is a naturally occurring antioxidant prevalent in both plant and animal foods, exhibiting bioactivity comparable to that of vitamins. Although its roles in antioxidant defense and metabolic regulation have been extensively studied, its potential to mitigate heat stress in organisms is less explored and deserves further study. Our research demonstrates that ALA significantly improves the survival rates of *Caenorhabditis elegans* under heat stress. ALA achieves this by activating heat shock factor 1 (HSF-1) and promoting mitochondrial fission and mitophagy through the transcription factor HLH-30. These processes help alleviate oxidative damage from heat stress, maintain mitochondrial function, and stabilize cellular energy metabolism. Furthermore, the activation of HSF-1 and enhanced mitophagy by dietary ALA depend on the insulin-like signaling peptide 19 (INS-19), suggesting that ALA may target the insulin-like signaling pathway to combat heat stress and maintain homeostasis. These findings indicate that ALA could serve as a valuable dietary supplement for enhancing heat stress resistance in organisms and may inspire the development of novel food ingredients with protective properties against thermal challenges.

Received 30th October 2024,
Accepted 27th February 2025

DOI: 10.1039/d4fo05301j

rsc.li/food-function

1 Introduction

With the escalation of global warming, the incidence of heat stress is increasing, leading to oxidative stress that may adversely affect various physiological functions and health aspects in organisms, such as lipid metabolism, intestinal barrier function, and reproductive health.[1–4] Animals possess various pathways to address environmental high-temperature challenges including oxidative stress, protein misfolding, and heat shock, enabling them to survive and thrive under such conditions.[5] Hence, enhancing thermoregulation and acclimatization through dietary means is an urgently needed alternative to traditional physical cooling methods.[6]

Alpha-lipoic acid (ALA), which is widely found in the diets of humans and animals, such as in beets, carrots, potatoes, spinach, broccoli, red meat, particularly in organ tissues with higher metabolic rates such as the heart, liver and kidneys, is a vital antioxidant and co-factor in the enzymatic digestion of nutrients. It significantly influences energy metabolism and boasts numerous biological benefits.[7,8] The body's natural capacity to synthesize ALA diminishes with age, underscoring the importance of dietary supplementation.[9] Furthermore, ALA is prominently involved in mitochondrial dehydrogenase reactions and has recently been recognized for its robust antioxidant properties.[10] Extensive research has explored its therapeutic potential in treating various oxidative stress-related conditions. By scavenging reactive oxygen species (ROS) and enhancing the availability of reduced glutathione (GSH), ALA effectively inhibits free radical formation, thereby maintaining cellular redox homeostasis. In addition to being safe as a dietary supplement in humans, ALA has been shown to have beneficial effects in several diseases characterized by oxidative stress.[10] However, whether and how ALA ameliorates heat stress to promote thermotolerance remains unknown.

Caenorhabditis elegans (*C. elegans*) is a classic model organism that exhibits disease pathway conservation in higher organisms owing to its small size (conducive to culture), short reproductive span, transparent body (for observing fluorescent markers),[11] and significant genomic similarities with higher animals.[12] This

[a]*College of Food Science, Fujian Agriculture and Forestry University, Fuzhou 350002, China. E-mail: zsxfst@163.com*
[b]*School of Agriculture and Biology, Shanghai Jiao Tong University, Shanghai 200240, China. E-mail: lingjunzheng@sjtu.edu.cn*
[c]*College of Tea and Food Science, Wuyi University, Wuyishan 354300, China*
†These authors contributed equally to this study.

high conservation between *C. elegans* and higher organisms, including humans, allows us to study the basic mechanisms of the heat stress response that may be shared across species. It also enables the screening and functional verification of high-throughput active compounds, making it a pivotal model for investigating stress defense and pathogenesis pathways.[13] Hence, the role and mechanism of ALA in alleviating heat stress can be further explored using *C. elegans*, providing insights into its impact on cellular health and disease progression.[14] Recent human studies have demonstrated that repeated exposure to heat stress induces alterations in gene expression associated with the heat shock response, as well as anti-apoptotic and anti-oxidative pathways.[15] These observations align with our findings in *C. elegans*, further suggesting the potential existence of a similar mechanism in humans.

Under heat stress, the heat shock response (HSR) is activated, leading to an increase in heat shock factors (HSFs). This, in turn, boosts the production of heat shock proteins (HSPs), which play a critical role in protecting cells by preventing protein damage and aggregation.[16,17] In addition, exposure to high temperatures elevates the body's metabolic rate. To meet the increased energy demands, mitochondria—the cell's primary energy producers—intensify their activity, ensuring the maintenance of cellular functions under stress conditions. During the metabolic process, mitochondria generate a large amount of ROS. When ROS production exceeds the clearance capacity of the body's antioxidant system, oxidative stress occurs. Therefore, heat stress is closely associated with oxidative stress and mitochondrial function. To adapt to heat stress, cells rapidly adjust mitochondrial number and morphology, while mitophagy enhances mitochondrial function to stabilize cellular metabolism.[18–20] It has been reported that inhibition of genes in the insulin-like signaling pathway can enhance heat resistance by activating FOXO transcription factors, which regulate protein homeostasis and antioxidant mechanisms.[21–23] Additionally, insulin-like peptides, produced by various cell types including neurons, may play a central role in stress response *via* the gut–brain axis.[24] Therefore, this study aimed to investigate the effects of ALA on the survival rate, protein homeostasis, and mitophagy involving the insulin-like pathway for promoting heat resistance in *C. elegans* under heat stress,[16,17] which could open up possibilities for further exploration of bioactive food compounds with potential applications.

2 Materials and methods

2.1 Chemicals and strains

The *C. elegans* strains N2 (wild-type strain), CF1038 [*daf-16 (mu86)* I], SJ4100 (zcIs13[*hsp-6p::GFP*] V), TJ356 (zIs356 [*daf-16p::daf-16a/b::GFP* + *rol-6(su1006)*] IV), CL2166 (dvIs19 [(pAF15)*gst-4p::GFP::NLS*] III), CF1553 (muIs84 [(pAD76) *sod-3p::GFP* + *rol-6 (su1006)*]), SJ4005 (zcIs4 [*hsp-4p::GFP*] V), CL2070 (dvIs70 [*hsp-16.2p::GFP* + *rol-6(su1006)*]), MAH240 (sqIs17 [*hlh-30p::hlh-30::GFP* + *rol-6(su1006)*]), MAH242 (sqIs24 [*rgef-1p::GFP::lgg-1* + *unc-122p::RFP*]), SJ4103 (zcIs14 [*Pmyo-3::GFP*(mit)]), SJ4143 (zcIs17 [*Pges-1::GFP*(mit)]), SJZ106 [*pie-1p::tomm-20::mKate2::HA::tbb-2 3′ UTR* I], MT7929 [*unc-13(e51)* I], CB928 [*unc-31(e928)* IV], PS3551 [*hsf-1(sy441)* I], and *Escherichia coli* OP50 bacteria, used to feed the nematodes, were provided by the Caenorhabditis Genetics Center. Lipoic acid (ALA) and all the compounds required to prepare the nematode growth media (NGM) were purchased from Sigma-Aldrich (St Louis, MO).

2.2 *C. elegans* maintenance and treatment

All strains were cultivated on *E. coli* OP50 using nematode growth media (NGM) at a temperature of 20 °C, following established protocols. The synchronization of cultures was achieved through either chemical treatment with sodium hypochlorite or manual selection of embryos.

ALA stock solution was prepared by dissolving ALA in DMSO. The experimental group received ALA (25 μM) added to the NGM medium with *E. coli* OP50, while the control group received the same volume of ddH_2O. To ensure that all worms were at identical developmental phases for consistency across experiments, synchronized eggs were cultured on NGM plates at 20 °C until they reached the young adult or early adult stage, prior to subjecting them to heat stress at 35 °C for 1 hour.

2.3 Thermotolerance assays

Synchronized eggs were raised to young adulthood at 20 °C and then exposed to 35 °C for 4.5 hours of heat stress treatment. For RNAi-mediated knockdown of genes, worms were transferred onto RNAi plates from the Ahringer library from the egg stage and maintained at 20 °C to young adulthood, followed by exposure to 35 °C heat stress for 4.5 hours. The survival of the worms was scored 24 hours later. Worms were scored as deceased if they failed to respond to gentle stimulation using an eyebrow hair. Individuals that burrowed into or escaped from the agar, or exhibited signs of mortality, were promptly removed during the enumeration process.

A minimum of three replicates was conducted for all experiments, with a cohort of over 50 worms per replicate. Experiments were conducted blindly in all cases.

2.4 RNAi feeding

The RNAi plate was prepared by adding ampicillin (final concentration 100 μg mL^{-1}) and isopropyl-β-D-thiogalactoside (IPTG) (final concentration 1 mM) to the NGM ordinary plate. Strains derived from the Ahringer library were cultivated in LB liquid medium supplemented with ampicillin (100 μg mL^{-1}) at 37 °C for an overnight period, after which they were transferred onto RNAi plates for further analysis. The worms were fed with *E. coli* HT115 containing an empty vector control or the designated RNAi bacteria was used.

2.5 Food preference

Synchronized eggs were cultivated on NGM plates with *E. coli* OP50 bacteria and developed to the young adult stage at a temperature of 20 °C. Food preference assay was performed on 90 mm NGM plates. Bacterial food with a diameter of 1 cm was seeded 1 cm away from the periphery. The control group consisted of *E. coli* OP50 cultured with water, represented in

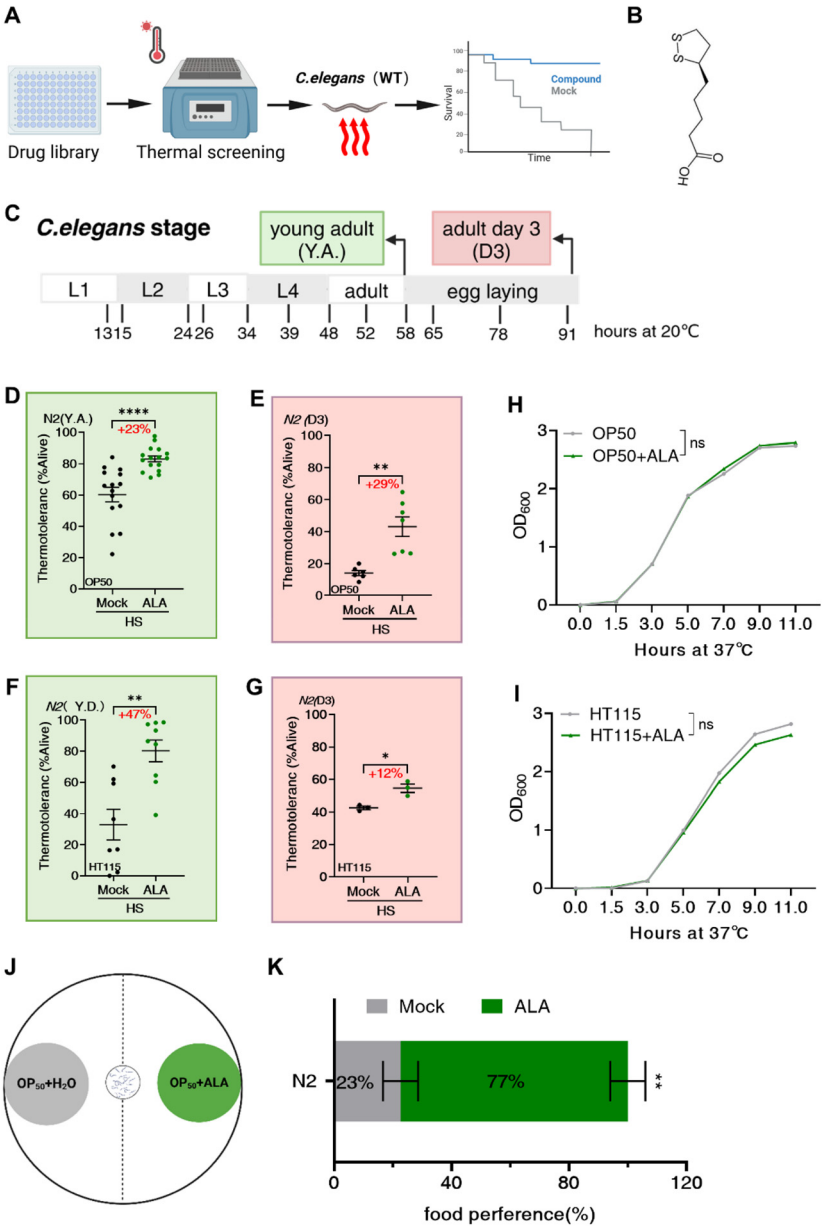

Fig. 1 ALA enhances heat resistance in *C. elegans*. (A) Schematic representation of natural product active ingredient screening for heat resistance using nematode models. (B) Schematic of the chemical structure of lipoic acid. (C) Different developmental stages of *C. elegans*. (D) Thermotolerance assay of young adulthood (Y.A.) N2 worms shifted from 20 °C to 35 °C for 4.5 hours heat stress treatment. Survival rates were measured 24 hours after recovery at 20 °C. Data are the mean ± SEM of ≤900 worms combined from three biological experiments. ****$p \leq 0.0001$ by Student's *t*-test. (E) Thermotolerance assay of adult day-3 N2 worms shifted from 20 °C to 35 °C for 4.5 hours heat stress treatment. Survival rates were measured 24 hours after recovery at 20 °C. Data are the mean ± SEM of ≤500 worms combined from three biological experiments. **$p \leq 0.01$ by Student's *t*-test. (F) Worms were exposed to control RNAi (*E. coli* HT115) plate with or without ALA beginning from egg to young adulthood (Y.A.). Thermotolerance assay of young adulthood (Y.A.) N2 worms shifted from 20 °C to 35 °C for 4.5 hours heat stress treatment. Survival rates were measured 24 hours after recovery at 20 °C. Data are the mean ± SEM of ≤600 worms combined from three biological experiments. **$p \leq 0.01$ by Student's *t*-test. (G) Worms were exposed to control RNAi (*E. coli* HT115) plates beginning from egg to adult day-3 with or without ALA. Thermotolerance assay of adult day-3 N2 worms shifted from 20 °C to 35 °C for 4.5 hours heat stress treatment. Survival rates were measured 24 hours after recovery at 20 °C. Data are the mean ± SEM of ≤200 worms combined from three biological experiments. *$p \leq 0.05$ by Student's *t*-test. (H) ALA does not alter the growth rate of *E. coli* OP50, which is the standard laboratory food source for nematodes. Bacterial cells from the same overnight OP50 culture were added to the LB ± ALA mixture at a 1 : 40 dilution, and then placed in the 37 °C incubator shaker at 300 rpm. The absorbance at 600 nm was read at 2 h time intervals to generate the growth curve. (I) ALA does not alter the growth rate of *E. coli* HT115, which is the standard laboratory food source for nematodes. Bacterial cells from the same overnight HT115 culture were added to the LB ± ALA mixture at a 1 : 40 dilution, and then placed in the 37 °C incubator shaker at 300 rpm The absorbance at 600 nm was read at 2 h time intervals to generate the growth curve. (J) Schematic representation of food preference assay (the gray area is *E. coli* OP50 treated with water as the control group, and the green area is *E. coli* OP50 treated with ALA as the experimental group). (K) Statistical chart of food preference assay. Worms show preference to *E. coli* OP50 food treated with ALA. **$p \leq 0.01$ by Student's *t*-test.

gray, while the experimental group, depicted in green, involves *E. coli* OP50 treated with ALA (Fig. 1J). Worms were placed at the center of the assay plate in order to facilitate their dispersal. Following a two-hour migration period, their distribution across the bacterial lawns was evaluated and quantified.

2.6 Measurement of autophagy levels

Autophagy was monitored by counting GFP-positive LGG-1 puncta in the nerve-ring neurons of strain MAH242. Worms were cultured at 20 °C until reaching adult day-1 (D1), then subjected to heat stress at 35 °C for 1 hour, followed by a 4-hour recovery period for fluorescence imaging. For puncta quantification, worms were anesthetized using 0.1% sodium azide on 3% agarose pads and GFP::LGG-1 foci were enumerated using a Nikon 80i fluorescence microscope.[16] To visualize the nerve-ring, a series of *Z*-stack images were captured with 0.6 μm intervals using an Olympus FV3000 confocal laser microscope at a magnification of 1024×.

2.7 Nuclear localization reporter gene expression

The visualization of HLH-30::GFP and DAF-16::GFP expression and nuclear localization was accomplished by capturing fluorescence images of worms immobilized on NGM agar with 0.1% sodium azide, using a Nikon 80i fluorescence microscope. To minimize the potential influence of external pressure on nuclear localization, imaging was conducted within a defined time frame of 5 minutes.

2.8 Microscopy and fluorescence imaging

Whole-body fluorescence intensity was measured on young adulthood in strains SJ4100, TJ356, CL2166, CF1553, SJ4005, CL2070, SJ4143, MAH240 raised at 20 °C and then maintained under control conditions or subjected to heat stress for 1 h at 35 °C followed by 6 h recovery.

Worms were anesthetized using 0.1% sodium azide and mounted onto 3% agarose pads for immobilization, before fluorescence imaging with a Nikon 80i microscope.

2.9 Fluorescence analysis

Fluorescence intensity analysis of individual worms was performed using ImageJ software from NIH (National Institutes of Health), involving the tracing of each worm's outline and quantification of mean GFP fluorescence intensity per worm. In three independent experiments, approximately 20 worms were subjected to imaging.

2.10 Analysis of mitochondria morphology

For worms expressing GFP-labeled muscle mitochondria (*Pmyo-3::mtGFP*), imaging was performed at the young adulthood stage. Strain SJZ106 was examined using D1 worms grown on *E. coli* OP50 at a standard temperature of 20 °C or subjected to heat stress for 1 hour at 35 °C. Subsequently, 2D imaging was conducted utilizing an Olympus FV3000 confocal laser scanning microscope.[25]

2.11 RNA sample preparation and RNA-seq

Approximately 12 000 to 15 000 synchronized worms were cultured at 20 °C. Three replicates were performed for RNA-seq. The control group was maintained at 20 °C, while the experimental group was exposed to 35 °C for 1 hour. After a 2-hour recovery period, samples were collected and rapidly frozen in liquid nitrogen and stored at −80 °C.

RNA extraction, cDNA synthesis, library preparation, and subsequent sequencing services were performed by Majorbio Bio-pharm Biotechnology Co., Ltd in Shanghai, China, following the guidelines provided by Illumina, San Diego, CA. Quantification of the RNA-seq libraries was conducted using the Qubit 4.0 fluorometer, and the libraries were then subjected to paired-end sequencing on a NovaSeq X Plus platform with a read length of 150 bp per end.

Raw paired-end reads were processed for quality control and trimming with 'fastp' utilizing its default parameters. Subsequently, the polished reads were aligned to the reference genome in a directional manner using the HISAT2 software.[26,27]

2.12 RNA-seq data analysis

Gene expression profiles were analyzed using DESeq2 or DEGseq to identify differential expression patterns between the ALA-treated group and the mock group under heat stress. DESeq2 was used for differential expression analysis of the two groups of samples. Differentially expressed genes (DEGs) with $|\log2FC| \geq 1$ and FDR < 0.05(DESeq2) were considered statistically significant. Heat stress-induced differential genes related to neurotransmitters and neuropeptides were visualized using heatmaps created with GraphPad Prism 9.5.

2.13 Statistics

Statistical comparisons of heat stress responses were performed using Student's *t*-test and two-way ANOVA. Fluorescence intensity data were analyzed using Student's *t*-test, and transcriptome data were analyzed using two-way ANOVA after confirming the normality of data distribution with GraphPad Prism 9.

3 Results

3.1 ALA enhances heat resistance in *C. elegans*

To identify food-derived active compounds that can enhance thermotolerance, we screened small-molecular compounds capable of alleviating heat stress in organisms (Fig. 1A). Worms were cultured under standard conditions and pretreated with various small-molecule compounds in the growth medium. They were then subjected to heat stress by exposure to elevated temperatures. Survival rates were carefully monitored and documented using a microscope. By comparing the treated groups with the control group, we identified compounds that significantly improve heat resistance. Specifically, lipoic acid, an eight-carbon fatty acid with sulfur atoms attached to carbons 6 and 8,[28] demonstrated promising results in increasing heat resistance in worms (Fig. 1B).

To assess the potential of ALA as a geroprotector, we conducted thermotolerance assays on worms at various developmental stages (Fig. 1C). Our results showed that administering ALA during the early adult phase led to a 23.0% increase in survival (Fig. 1D). Additionally, ALA significantly improves heat resistance in aged worms at adult day-3 (Fig. 1E). To explore whether metabolites from OP50 enhance heat resistance, we evaluated the impact of various *E. coli* strains on thermotolerance assays. Remarkably, ALA improved heat resistance in worms regardless of whether they consumed *E. coli* OP50 or HT115, with no significant differences observed between the two bacterial strains (Fig. 1F and G).

Fasting is widely recognized for enhancing heat resistance in diverse organisms. We investigated the effects of ALA-induced fasting on bacterial growth and its potential to repel worms. Specifically, we tested the effect of ALA on the growth of two *E. coli* strains, OP50 and HT115, by evaluating their metabolic activity after treatment. Our results indicated that ALA had minimal impact on the growth of both *E. coli* strains (Fig. 1H and I). Furthermore, observations of worm behavior towards ALA-treated *E. coli* showed no signs of avoidance, suggesting that ALA does not act as a repellent (Fig. 1J and K). These results collectively indicate that the heat resistance conferred by ALA in *C. elegans* is not mediated through effects on bacterial growth, metabolic activity, or food intake. Instead, our findings suggest a direct mechanism through which ALA enhances heat resistance within the worms themselves, independent of indirect impacts involving bacterial interactions.

3.2 ALA-mediated heat resistance is required for DAF-16

To gain insights into the molecular mechanisms underlying ALA-mediated heat resistance, we first assessed the expression of DAF-16, a protein associated with stress resistance. We quantitatively evaluated the nuclear accumulation of DAF-16::GFP in the intestine under heat stress to measure the level of thermal stress response. DAF-16, analogous to the Forkhead box O (FOXO) family in humans, plays a pivotal role in regulating various biological processes like longevity and stress resistance. Within the cell nucleus, DAF-16 functions independently or in conjunction with other transcription factors such as heat shock factor-1 (HSF-1) and skinhead-1 (SKN-1) to regulate a variety of stress-responsive genes, including superoxide dismutase SOD-3, glutathione s-transferase GST-4, and the heat shock protein HSP-16.2 (Fig. 2A).[29] Consistent with this, we observed the translocation of DAF-16 to the nucleus after heat stress in both ALA-treated and control conditions (Fig. 2B–D). Notably, ALA treatment did not significantly enhance the nuclear translocation of the DAF-16 protein (Fig. 2E). However, upon knockout of the *daf-16* gene, ALA failed to enhance heat resistance (Fig. 2F), highlighting the essential role of *daf-16* in this process. Additionally, we observed no response from the antioxidant genes *sod-3* and *gst-4* to heat stress (Fig. 2G–J), further emphasizing the unique role of DAF-16 in this mechanism. Collectively, our findings demonstrate that ALA enhances heat resistance through a pathway involving DAF-16, while other antioxidant genes do not appear to contribute significantly to this process, underscoring the pivotal role of DAF-16 in mediating the heat resistance effects of ALA.

3.3 ALA activates HSF-1 to promote heat resistance

To explore the molecular mechanisms underlying ALA-induced heat resistance, we performed epistasis experiments to assess the role of heat shock factor-1 (HSF-1). We focused on a *C. elegans* strain (PS3551) carrying a missense mutation that produces a truncated, nonfunctional HSF-1 protein (Fig. 3A). Our results demonstrated that ALA did not enhance heat resistance in worms with this defective HSF-1 protein (Fig. 3B), indicating that ALA-induced heat resistance depends, at least in part, on HSF-1, the key transcription factor for stress protein induction. To further investigate HSF-1's role in ALA-induced heat resistance, we analyzed the effects of ALA on the expression of downstream targets of HSF-1, specifically HSP-4 and HSP-16.2.[30,31]

Following exposure to heat stress, we observed a significant increase in whole-body expression of HSP-4::GFP (Fig. 3C–F) and a marked upregulation of HSP-16.2::GFP expression (Fig. 3G–J). These proteins are typically expressed at low levels under normal conditions. Notably, ALA treatment further enhanced the expression of these molecular chaperones, HSP-4 and HSP-16.2 (Fig. 3K and L). These findings support the hypothesis that ALA activates HSF-1 to enhance heat resistance. Importantly, heat stress specifically induced the expression of the ER UPR reporter *hsp-4p::GFP* and the cytosolic UPR reporter *hsp-16.2p:: GFP*, while leaving the mitochondrial UPR unaffected (Fig. 3M and N).

3.4 ALA-mediated heat resistance through inducing autophagy

HSF-1 is a key regulator of autophagy induction under thermal stress. When cells encounter stressful conditions, autophagy is initiated, leading to the formation of autophagosomes that engulf damaged cytoplasmic structures. These autophagosomes subsequently fuse with lysosomes, where their contents are degraded by hydrolases and recycled. Unlike the heat shock response (HSR), autophagy is a more efficient process for handling large protein aggregates and malfunctioning organelles caused by heat stress. Recent studies have demonstrated that thermal stress activates autophagy. Specifically, research has shown the global activation of autophagy in *C. elegans* through an HSF-1-dependent process during heat stress. Furthermore, autophagy-related genes play a critical role in the increased autophagosome formation observed in worms following heat stress.[32,33]

The transcription factor HLH-30, the *C. elegans* homolog of mammalian TFEB, is essential for various organismal functions, including heat resistance, with its transcriptional activity dependent on nuclear translocation.[34–36] Under heat stress conditions, we observed rapid translocation of GFP-tagged HLH-30 into the nucleus across multiple tissues, including the nerve ring, pharynx, vulva, tail, and intestine (Fig. 4A–D). Additionally, our findings indicate that ALA enhances this nuclear translocation of HLH-30, thereby increasing its transcriptional activity in response to ALA (Fig. 4E). As the homolog of the mammalian TFEB, HLH-30 plays a pivotal role

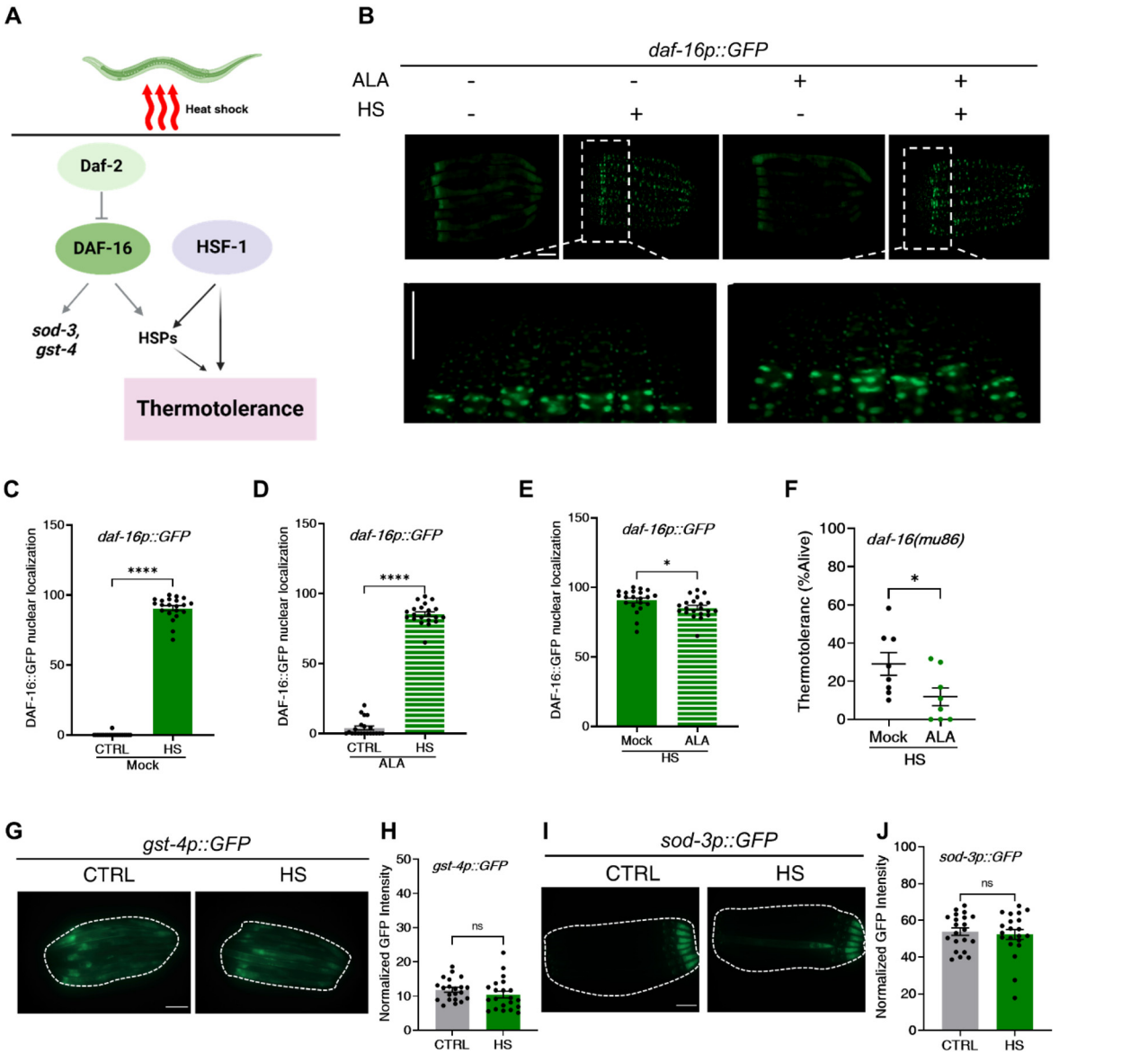

Fig. 2 ALA-mediated heat resistance is required for DAF-16. (A) Thermotolerance pathway schematic. (B) Representative microphotographs of *daf-16p::GFP* worms, with ALA treatment, under two conditions: (1) control conditions (20 °C, CTRL), and (2) following 1 hour of heat stress at 35 °C (HS). Regions of GFP-marked are shown in enlarged insets, scale bar = 100 μm. (C) Quantification of GFP fluorescence from strains used in (B: comparison between control and heat stress without ALA). Data are the mean ± SEM of ≤30 worms combined from three biological experiments. ****$p \leq 0.0001$ by Student's *t*-test. (D) Quantification of GFP fluorescence from strains used in (B: comparison between control and heat stress with ALA). Data are the mean ± SEM of ≤30 worms combined from three biological experiments. ****$p \leq 0.0001$ by Student's *t*-test. (E) Quantification of GFP fluorescence from strains used in (B: comparison between Mock group and ALA group under heat stress condition). Data are the mean ± SEM of ≤30 worms combined from three biological experiments. *$p \leq 0.05$ by Student's *t*-test. (F) Thermotolerance assay of *daf-16(mu86)* worms shifted from 20 °C to 35 °C for 4.5 hours heat stress treatment. Survival rates were measured 24 hours after recovery at 20 °C. Data are the mean ± SEM of ≤500 worms combined from three biological experiments. *$p \leq 0.05$ by Student's *t*-test. (G) Representative microphotographs of *gst-4p::GFP* worms under two conditions: (1) control conditions (20 °C, CTRL), and (2) following 1 hour of heat stress at 35 °C (HS). Scale bar = 100 μm. (H) Quantification of GFP fluorescence from strains used in (G). Data are the mean ± SEM of ≤30 worms combined from three biological experiments. $p > 0.05$ by Student's *t*-test. (I) Representative microphotographs of *sod-3p::GFP* worms under two conditions: (1) control conditions (20 °C, CTRL), and (2) following 1 hour of heat stress at 35 °C (HS). Scale bar = 100 μm. (J) Quantification of GFP fluorescence from strains used in (I). Data are the mean ± SEM of ≤30 worms combined from three biological experiments. $p > 0.05$ by Student's *t*-test.

in autophagy and lysosomal activation upon heat stress, underscoring its regulatory influence on heat stress-induced autophagy[37] (Fig. 4F). We also observed an increase in GFP::LGG-1/Atg8 puncta in nerve ring neurons, demonstrating that ALA promotes autophagosome formation in neurons (Fig. 4G–J). Our study revealed that ALA enhances autophagosome formation in worm neurons (Fig. 4K). To investigate whether ALA-mediated thermotolerance depends on autophagy or mito-

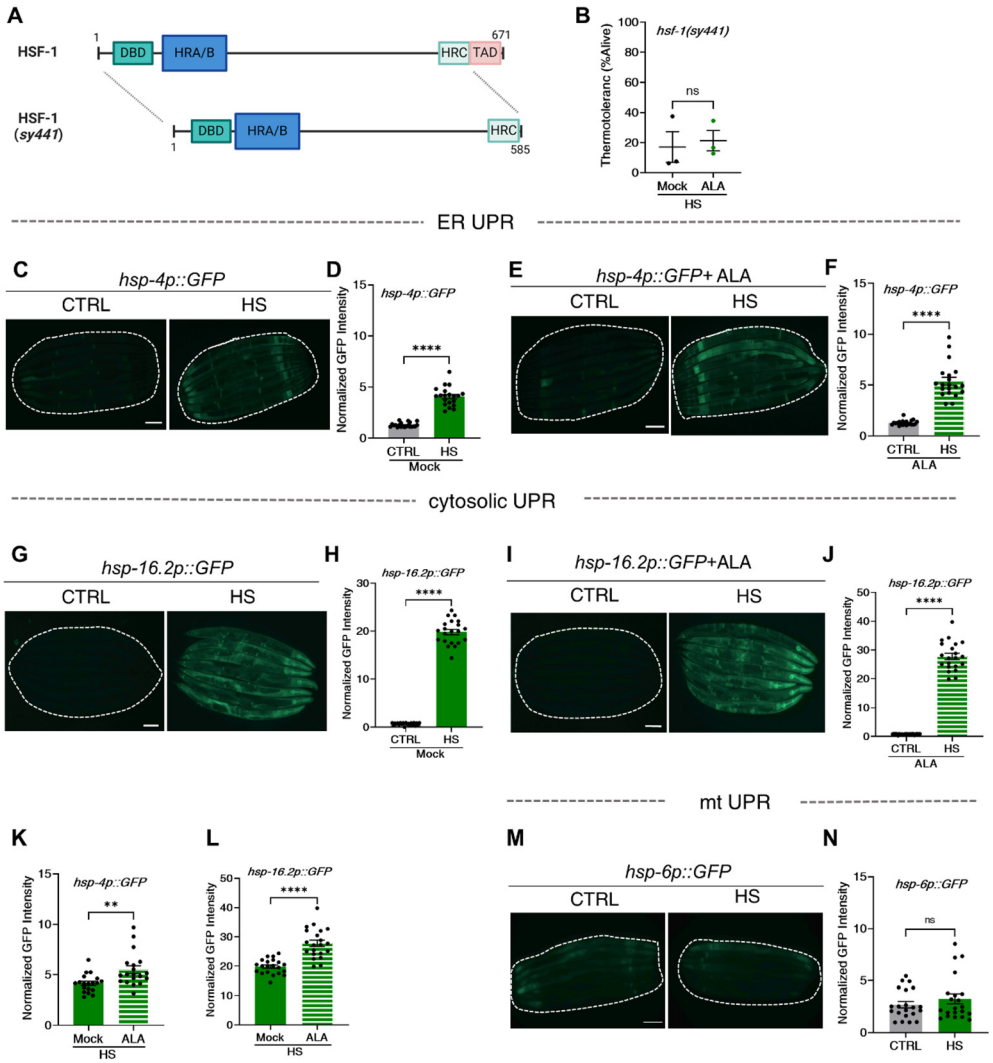

Fig. 3 ALA activates HSF-1 to promote heat resistance. (A) Domain structure of *C. elegans* HSF-1 full-length protein and the truncated alleles *sy441*. Numbers indicate amino acid positions. DBD is the DNA-binding domain, HR-A/B and HR-C are the trimerization domains and TAD is the transactivation domain. HSF-1 trimerization is negatively regulated by intramolecular interactions between the HR-A/B and the HR-C domains. The exact position of the regulatory domain in the *C. elegans* HSF-1 is not yet determined. However, it is most possibly located between the two trimerization domains and negatively regulates the trans-activating capacity of HSF-1. *sy441* allele is lacking the transactivation domain. (B) Thermotolerance assay of *hsf-1(sy441)* worms shifted from 20 °C to 35 °C for 4.5 hours heat stress treatment. Survival rates were measured 24 hours after recovery at 20 °C. Data are the mean ± SEM of ≤200 worms combined from three biological experiments. $p > 0.05$ by Student's *t*-test. (C) Representative microphotographs of *hsp-4p::GFP* worms under two conditions: (1) control conditions (20 °C, CTRL), and (2) following 1 hour of heat stress at 35 °C (HS) and a subsequent 6-hour recovery period. Scale bar = 100 μm. (D) Quantification of GFP fluorescence from strains used in (C). Data are the mean ± SEM of ≤30 worms combined from three biological experiments. ****$p \leq 0.0001$ by Student's *t*-test. (E) Representative microphotographs of *hsp-4p::GFP* worms, with ALA treatment, under two conditions: (1) control conditions (20 °C, CTRL), and (2) following 1 hour of heat stress at 35 °C (HS) and a subsequent 6-hour recovery period. Scale bar = 100 μm. (F) Quantification of GFP fluorescence from strains used in (E). Data are the mean ± SEM of ≤30 worms combined from three biological experiments. ****$p \leq 0.0001$ by Student's *t*-test. (G) Representative microphotographs of *hsp-16.2p::GFP* worms under two conditions: (1) control conditions (20 °C, CTRL), and (2) following 1 hour of heat stress at 35 °C (HS) and a subsequent 6-hour recovery period. Scale bar = 100 μm. (H) Quantification of GFP fluorescence from strains used in (G). Data are the mean ± SEM of ≤30 worms combined from three biological experiments. ****$p \leq 0.0001$ by Student's *t*-test. (I) Representative microphotographs of *hsp-16.2p::GFP* worms, with ALA treatment, under two conditions: (1) control conditions (20 °C, CTRL), and (2) following 1 hour of heat stress at 35 °C (HS) and a subsequent 6-hour recovery period. Scale bar = 100 μm. (J) Quantification of GFP fluorescence from strains used in (I). Data are the mean ± SEM of ≤30 worms combined from three biological experiments. ****$p \leq 0.0001$ by Student's *t*-test. (K) Quantification of GFP fluorescence from strains used in (C and E: with and without ALA treatment). The two groups of experiments in Figure C and E were carried out at the same time, using the same batch of worms. Data are the mean ± SEM of ≤30 worms combined from three biological experiments. **$p \leq 0.01$ by Student's *t*-test. (L) Quantification of GFP fluorescence from strains used in (G and I: with and without ALA treatment). The two groups of experiments in G and I were carried out at the same time, using the same batch of worms. Data are the mean ± SEM of ≤30 worms combined from three biological experiments. ****$p \leq 0.0001$ by Student's *t*-test. (M) Representative microphotographs of *hsp-6p::GFP* worms under two conditions: (1) control conditions (20 °C, CTRL), and (2) following 1 hour of heat stress at 35 °C (HS). Scale bar = 100 μm. (N) Quantification of GFP fluorescence from strains used in (N). Data are the mean ± SEM of ≤30 worms combined from three biological experiments. $p > 0.05$ by Student's *t*-test.

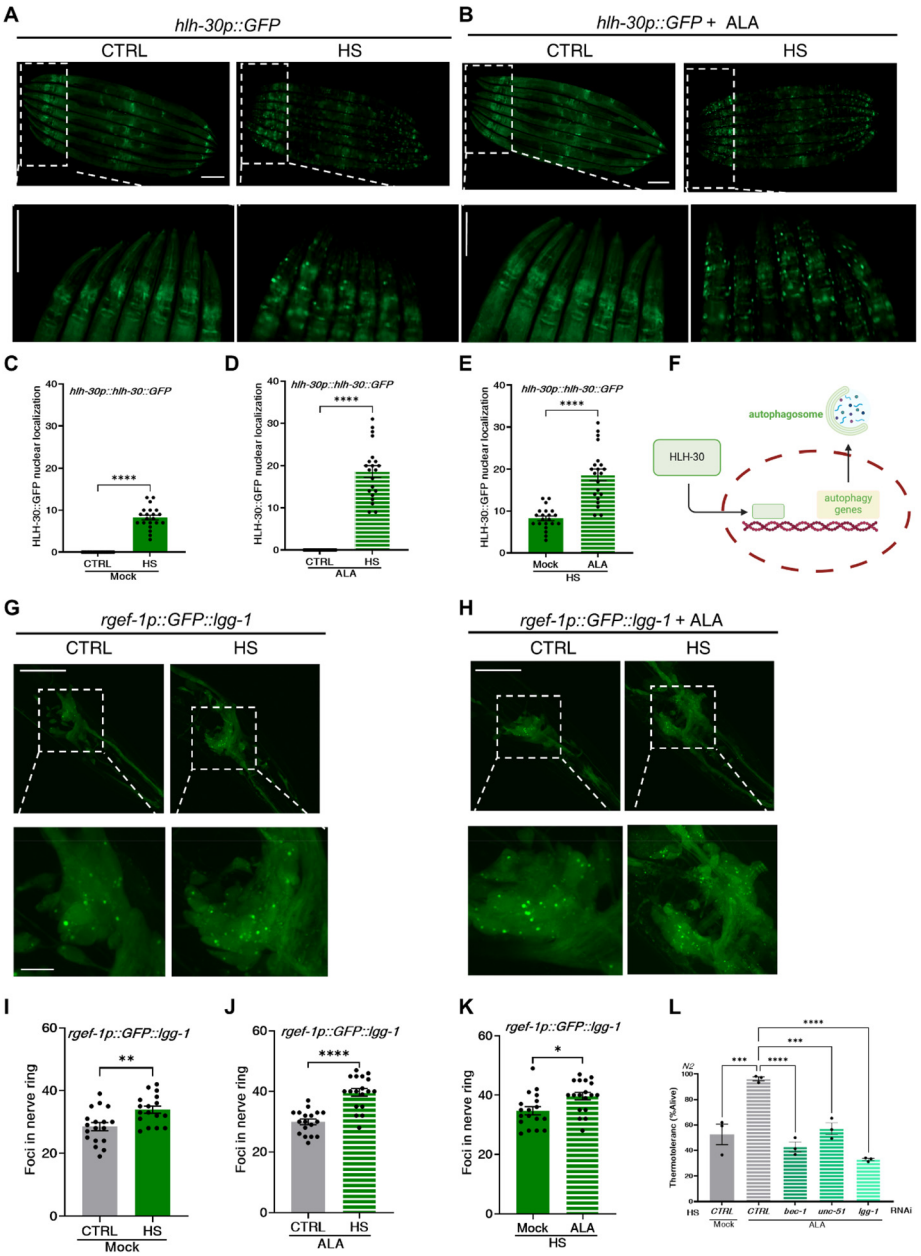

Fig. 4 ALA-mediated heat resistance through inducing autophagy. (A) Representative microphotographs of *hlh-30p::hlh-30::GFP* worms under two conditions: (1) control conditions (20 °C, CTRL), and (2) following 1 hour of heat stress at 35 °C and a subsequent 6-hour recovery period (HS). Scale bar = 100 μm. Regions of GFP-marked head are shown in enlarged insets (dotted white line). (B) Representative microphotographs of *hlh-30p::hlh-30::GFP* worms, with ALA treatment, under two conditions: (1) control conditions (20 °C, CTRL), and (2) following 1 hour of heat stress at 35 °C and a subsequent 6-hour recovery period (HS). Scale bar = 100 μm. Regions of GFP-marked head are shown in enlarged insets (dotted white line). (C) Quantification of GFP fluorescence from strains used in (A). Data are the mean ± SEM of ≤30 worms combined from three biological experiments. ****$p \leq 0.0001$ by Student's *t*-test. (D) Quantification of GFP fluorescence from strains used in (B). Data are the mean ± SEM of ≤30 worms combined from three biological experiments. ****$p \leq 0.0001$ by Student's *t*-test. (E) Quantification of GFP fluorescence from strains used in (A and B: with and without ALA treatment). Data are the mean ± SEM of ≤30 worms combined from three biological experiments. ****$p \leq 0.0001$ by Student's *t*-test. (F) Diagram of the mechanism of autophagy induced by transcription factor HLH-30 into the nucleus. (G) GFP::LGG-1/Atg8 puncta were counted in *rgef-1p::GFP::lgg-1* worms under two conditions: (1) control conditions (20 °C, CTRL), and (2) following 1 hour of heat stress at 35 °C, and a subsequent 4-hour recovery period (HS). Scale bar = 50 μm, enlarged insets scale bar = 10 μm. Puncta were examined in nerve ring neurons. (H) GFP::LGG-1/Atg8 puncta were counted in *rgef-1p::GFP::lgg-1* worms under two conditions, both with ALA treatment: (1) control conditions (20 °C, CTRL), and (2) following 1 hour of heat stress at 35 °C and a subsequent 4-hour recovery period (HS). Scale bar = 50 μm, enlarged insets scale bar = 10 μm. Puncta were examined in nerve ring neurons. (I) GFP::LGG-1 puncta were quantified in (G) ($N \leq 20$ worms). Data are the mean ± SEM. **$p \leq 0.01$ by Student's *t*-test. (J) GFP::LGG-1 puncta were quantified in (H) ($N \leq 20$ worms). Data are the mean ± SEM. ****$p \leq 0.0001$ by Student's *t*-test. (K) GFP::LGG-1 puncta were quantified in (G and H: with and without ALA treatment) ($N \leq 20$ worms). Data are the mean ± SEM. *$p \leq 0.05$ by Student's *t*-test. (L) Thermotolerance assay of *unc-51, bec-1 and lgg-1 RNAi-treated* N2 worms shifted from 20 °C to 35 °C for 4.5 hours heat stress treatment. Data are the mean ± SEM of ≤200 worms combined from three biological experiments. ***$p \leq 0.001$, ****$p \leq 0.0001$ by two-way ANOVE.

phagy, we knocked down autophagy-related genes *unc-51*, *bec-1*, and *lgg-1* using RNAi. Our results confirm that ALA-enhanced heat resistance relies on both autophagy and mitophagy (Fig. 4L), the latter being a targeted process for the removal of damaged mitochondria through autophagosome engulfment and lysosomal degradation.

3.5 ALA does not impact mitochondrial content after heat stress

A consistent feature of many stress responses is the disruption of mitochondrial content regulation within cells.[38,39] Given the role of mitophagy in ALA-enhanced heat resistance, we aimed to investigate the impact of ALA on mitochondrial quantity following heat stress. Using the intestinal promoter *ges-1* and the gonadal promoter *pie-1* to drive mtGFP, we quantified mitochondrial content in these tissues under heat stress conditions. These animals express GFP fused to a mitochondrial import signal in their intestines, resulting in well-organized mitochondrial arrays. Following heat stress, we observed an increase in the total mitochondrial quantity within the intestine (Fig. 5A–D). However, ALA treatment did not alter the overall mitochondrial quantity (Fig. 5E). Similar findings were confirmed using the *pie-1p::tomm-20::mKate2* germline mitochondrial reporter strain (Fig. 5F–J). Thus, heat stress leads to an increase in overall mitochondrial quantity, but ALA does not affect mitochondrial quantity in the intestine or germline after heat stress.

3.6 ALA induces mitochondrial fragmentation and mitophagy to enhance heat resistance

Although ALA does not alter the overall quantity of mitochondria in response to heat stress, it is noteworthy that heat stress induces a significant increase in mitochondrial fragmentation within muscle tissues, a process essential for the heat resistance. The transcription factor HLH-30/TFEB plays a critical role in mediating this fragmented state, thereby enhancing heat resistance. Therefore, we investigated the impact of ALA on mitochondrial fragmentation. Given the accessibility of muscle mitochondria for observation, we utilized this model to explore the underlying mechanisms. By analyzing mitochondrial morphology using a GFP-tagged mitochondrial reporter (mito::GFP) targeted to body wall muscles[40] (Fig. 6A and B), we assessed conditions with and without ALA. Our findings indicate that ALA promotes mitochondrial fission during thermal stress, suggesting its potential role in enhancing cellular resilience against heat-induced stress (Fig. 6C). Transcriptome analysis further revealed that ALA promotes mitochondrial fission following heat stress (Fig. 6D and E).

Additionally, the enhancement of heat resistance by ALA was associated with mitochondrial fragmentation, as evidenced by the reduced expression of the *drp-1* gene, which led to decreased survival rates for wild-type worms when subjected to heat stress (Fig. 6F). These findings underscore the crucial role of mitochondrial fragmentation in ALA-mediated heat stress protection. Collectively, our results propose that ALA enhances heat resistance by stimulating mitochondrial fragmentation and mitophagy, rather than by elevating mitochondrial numbers.

3.7 ALA actives HSF-1 and HLH-30 through INS-19

Coordinating stress responses across various tissues is essential for the survival of multicellular organisms. Upon exposure to heat stress, neurons play a pivotal role by releasing neurotransmitters that trigger a comprehensive heat shock response (HSR). Moreover, neuronal overexpression of the canonical HSR transcription factor, heat shock factor 1 (HSF-1), has been shown confer resistance to heat stress. These findings highlight the critical role of neurons in orchestrating and regulating organism-wide stress responses, emphasizing the importance of understanding inter-tissue interactions in heat stress adaptation.

It has been suggested that ALA may function by modulating neurotransmission or neurosecretion signaling. To explore this, we analyzed the effects of loss-of-function mutations *unc-13(e51)* and *unc-31(e928)*, which are known to impair synaptic vesicle (SCV) and dense core vesicle (DCV) release, respectively[41,42] (Fig. 7A). Our results showed that disruptions in SCV or DCV release did not enhance the heat resistance conferred by ALA (Fig. 7B and C), suggesting that neurosecretory events may actually hinder the heat resistance effects enhanced by ALA. To identify specific neuroendocrine signaling factors, we used transcriptomic analyses and found that ALA stimulates the transcription of the insulin-like signaling peptides *ins-19* during heat stress (Fig. 7D and E). Insulin-like signaling peptides are vital for regulating physiological responses under stress, helping organisms maintain homeostasis. This discovery led us to hypothesize that ALA activates HLH-30 and HSF-1 through the activation of *ins-19*. To test this hypothesis, we performed RNA interference targeting *ins-19*, and observed that ALA could no longer increase HSP-16.2::GFP expression or promote the nuclear translocation of HLH-30 following heat stress (Fig. 7F–I). Additionally, ALA failed to enhance heat resistance after RNA interference with *ins-19* (Fig. 7J). Our findings indicate that ALA modulates *ins-19* to activate HLH-30 and HSF-1, thereby regulating mitophagy and protein homeostasis, ultimately enhancing the organism's heat resistance (Fig. 7K).

4 Discussion

Heat stress can disrupt cellular function and lead to the accumulation of unfolded proteins, a condition linked to the onset and progression of various diseases.[43,44] The heat shock response (HSR) is a critical protective mechanism that involves upregulation of heat shock factors (HSFs), which subsequently enhance the production of heat shock proteins (HSPs) to prevent protein damage and aggregation.[16,17] Our study found that ALA induces HSR in *C. elegans* simultaneously promoted autophagy and mitochondrial fragmentation, which are conserved across species. A similar mechanism has been observed in mammalian pigs, where ALA restored the development and

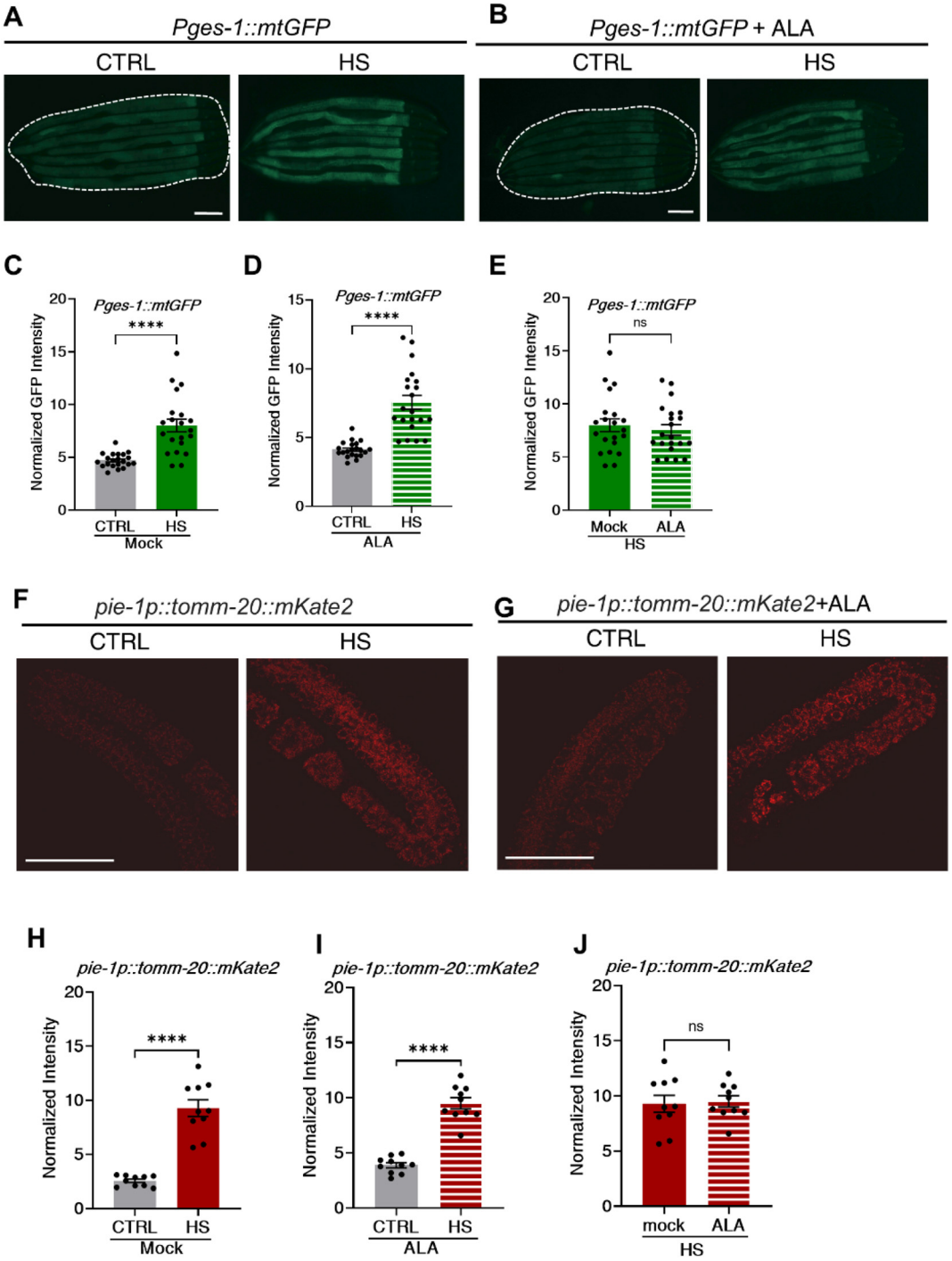

Fig. 5 ALA does not impact mitochondrial content after heat stress. (A) Representative images of intestinal mitochondrial morphology. *Pges-1::mtGFP* worms under two conditions: (1) control conditions (20 °C, CTRL), and (2) following 1 hour of heat stress at 35 °C and a subsequent 6-hour recovery period (HS). Scale bar = 100 μm. (B) Representative images of intestinal mitochondrial morphology. *Pges-1::mtGFP* worms, with ALA treatment, under the following conditions: (1) control conditions (20 °C, CTRL), and (2) following 1 hour of heat stress at 35 °C and a subsequent 6-hour recovery period (HS). Scale bar = 100 μm. (C) Quantification of GFP fluorescence from strains used in (A). Data are the mean ± SEM of ≤30 worms combined from three biological experiments. ****$p \leq 0.0001$ by Student's *t*-test. (D) Quantification of GFP fluorescence from strains used in (B). Data are the mean ± SEM of ≤30 worms combined from three biological experiments. ****$p \leq 0.0001$ by Student's *t*-test. (E) Quantification of GFP fluorescence from strains used in (A and B: with and without ALA treatment). Data are the mean ± SEM of ≤30 worms combined from three biological experiments. $p > 0.05$ by Student's *t*-test. (F) Fluorescence confocal imaging of *pie-1p::tomm-20::mKate2* germline mitochondrial reporter strain. Scale bar = 50 μm. (G) Fluorescence confocal imaging of *pie-1p::tomm-20::mKate2* germline mitochondrial reporter strain with ALA treatment. Scale bar = 50 μm. (H) Quantification of GFP fluorescence from strains used in (F). Data are the mean ± SEM. ****$p \leq 0.0001$ by Student's *t*-test. (I) Quantification of GFP fluorescence from strains used in (G). Data are the mean ± SEM. ****$p \leq 0.0001$ by Student's *t*-test. (J) Quantification of GFP fluorescence from strains used in (F and G: with and without ALA treatment) ($N = 10$ worms). Data are the mean ± SEM. $p > 0.05$ by Student's *t*-test.

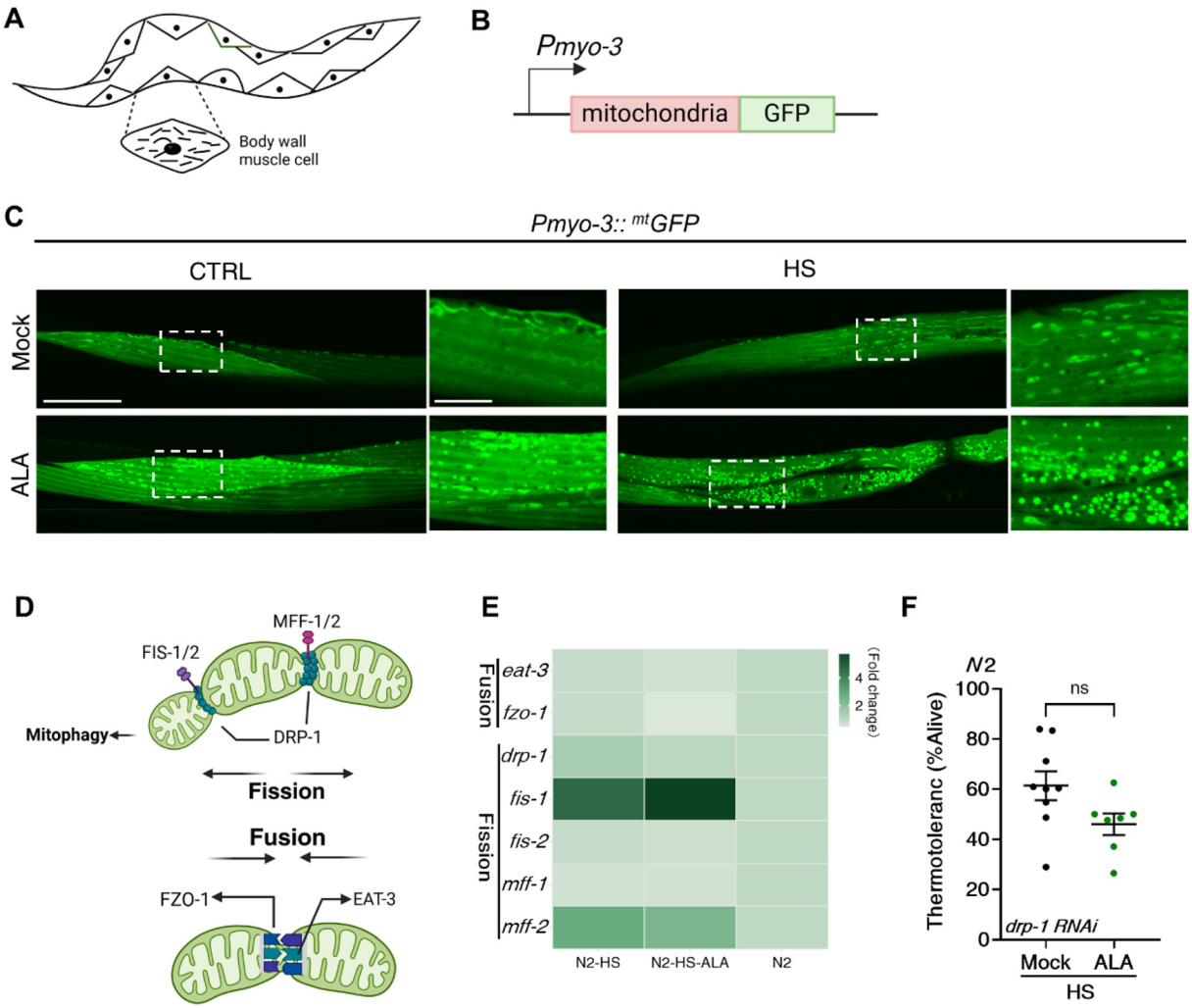

Fig. 6 ALA induces mitochondrial fragmentation and mitophagy to improve heat resistance. (A) Representative images of muscle mitochondrial morphology. (B) Domain structure of *Pmyo-3::mtGFP*. (C) Representative confocal images of muscle mitochondrial morphology. *Pmyo-3::mtGFP* worms were divided into four groups: (1) maintained at 20 °C without ALA, (2) maintained at 20 °C with ALA, (3) subjected to 1 hour of heat stress at 35 °C without ALA, and (4) subjected to 1 hour of heat stress at 35 °C with ALA. Scale bar = 12.5 μm, enlarged insets scale bar = 3.125 μm. (D) Schematic diagram of mitochondrial fusion division. (E) Transcript levels of Mitochondrial fusion fission genes in wild-type worms maintained at control conditions (20 °C, CTRL) or following 1 h of heat stress at 35 °C (HS). Normalized association values indicated by heatmap. (F) Thermotolerance assay of *drp-1* RNAi-treated N2 worms shifted from 20 °C to 35 °C for 4.5 hours heat stress treatment. Data are the mean ± SEM of ≤500 worms combined from three biological experiments. $p > 0.05$ by Student's *t*-test.

improved the quality of blastocysts at high temperatures and alleviates heat stress-induced apoptosis by upregulating the heat shock response.[45]

We investigated how ALA promotes heat resistance in *C. elegans*. Our findings reveal that ALA enhances heat resistance through a direct mechanism, rather than impacting bacterial development or metabolic activity. This excludes the possibility that ALA acts by altering bacterial populations or functioning as a food aversion agent. The heat resistance conferred by ALA is closely associated with key transcription factors, including DAF-16 and HSF-1. Although ALA treatment did not directly promote the nuclear translocation of the transcription factor DAF-16, the loss of the *daf-16* gene completely abolished ALA-induced thermotolerance. This indicates that DAF-16 is required for ALA to enhance heat resistance, even though ALA does not directly facilitate the nuclear translocation of DAF-16. This apparent discrepancy can be explained by considering the multifaceted nature of DAF-16's activity. DAF-16, a FOXO transcription factor, is involved in various stress response pathways and can exert its effects through mechanisms beyond nuclear translocation. For instance, DAF-16 can influence gene expression through interactions with other transcription factors. It has been shown that HLH-30 and the FOXO transcription factor DAF-16 form a complex that co-regulates the expression of numerous genes. However, whether this complex forms in the cytoplasm or nucleus, and whether DAF-16 influences HLH-30 subcellular transport, remains unclear.[34,46] Additionally, ALA may

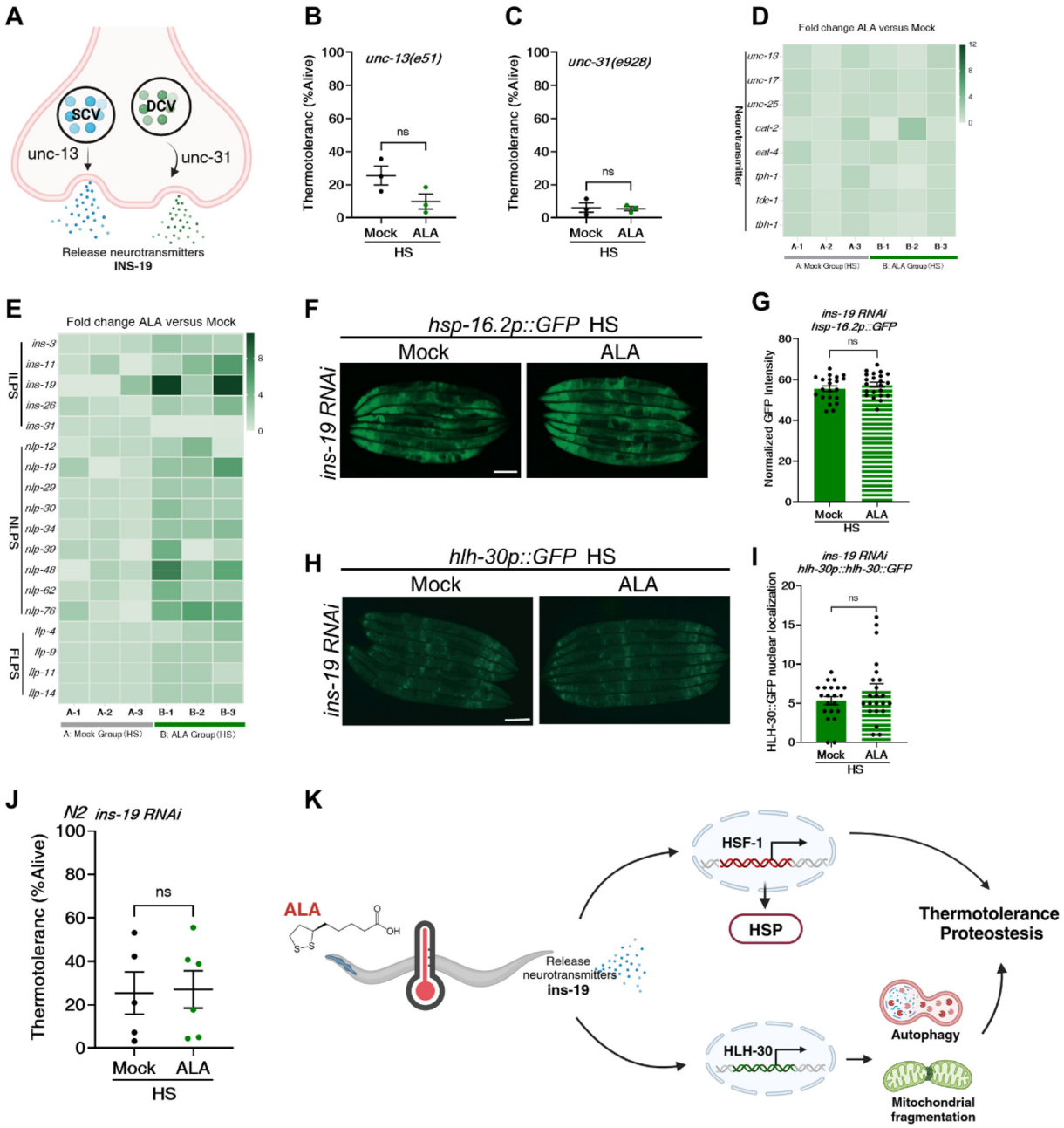

Fig. 7 ALA actives HSF-1 and HLH-30 through INS-19. (A) Map of neurotransmitter release pathway. (B) Thermotolerance assay of *unc-13(e51)* mutant strain shifted from 20 °C to 35 °C for 4.5 hours heat stress treatment. Survival rates were measured 24 hours after recovery at 20 °C. Data are the mean ± SEM of ≤200 worms combined from three biological experiments. $p > 0.05$ by Student's *t*-test. (C) Thermotolerance assay of *unc-31 (e928)* mutant strain shifted from 20 °C to 35 °C for 4.5 hours heat stress treatment. Survival rates were measured 24 hours after recovery at 20 °C. Data are the mean ± SEM of ≤200 worms combined from three biological experiments. $p > 0.05$ by Student's *t*-test. (D) Transcript levels of neurotransmitter genes in wild-type worms maintained under control conditions (20 °C, CTRL), or following 1 h of heat stress at 35 °C (HS). Normalized association values indicated by heatmap. (E) Transcript levels of neurotransmitter genes in N2 worms maintained at control conditions (20 °C, CTRL) or following 1 h of heat stress at 35 °C (HS). Normalized association values indicated by heatmap. (F) Representative microphotographs of *ins-19* RNAi-*treated hsp-16.2p::GFP* worms, which with and without ALA treatment, after being subjected to 1 hour of heat stress at 35 °C (HS) followed by a 6-hour recovery period. Scale bar = 100 μm. (G) Quantification of GFP fluorescence from strains used in (F). Data are the mean ± SEM of ≤30 worms combined from three biological experiments. $p > 0.05$ by Student's *t*-test. (H) Representative microphotographs of *ins-19* RNAi-*treated hlh-30p::hlh-30::GFP* worms, which with and without ALA treatment, following 1 h of heat stress at 35 °C (HS) and recover 6 hours. Scale bar = 100 μm. (I) Quantification of GFP fluorescence from strains used in (H). Data are the mean ± SEM of ≤30 worms combined from three biological experiments. $p > 0.05$ by Student's *t*-test. (J) Thermotolerance assay of *ins-19* RNAi-*treated* N2 worms shifted from 20 °C to 35 °C for 4.5 hours heat stress treatment. Data are the mean ± SEM of ≤400 worms combined from three biological experiments. $p > 0.05$ by Student's *t*-test. (K) Mechanism diagram of ALA promoting heat resistance of *C. elegans*.

indirectly modulate DAF-16 activity by affecting upstream signaling pathways that regulate DAF-16, such as the insulin/IGF-1 signaling pathway.[47,48]

As a key regulator of cellular stress responses, HSF-1 is well-known for orchestrating the expression of HSPs. Our experimental results demonstrate that ALA upregulates the expression of HSP-4 and HSP-16.2 through the HSF-1 transcription factor. In addition to regulating HSPs, HSF-1 enhances cellular antioxidant defenses, minimizing damage from mitochondria-derived reactive oxygen species (ROS) and protecting organelles from oxidative stress. Beyond these roles, HSF-1 plays a critical role in managing mitochondrial biogenesis and dynamics, including fusion and fission processes essential for maintaining mitochondrial quantity and function. Through these diverse mechanisms, HSF-1 coordinates the maintenance of mitochondrial homeostasis, ensuring efficient cellular energy metabolism, contributing significantly to cellular health, and supporting organismal survival.[16,33] Therefore, ALA may enhance heat tolerance through an HSF-1-dependent mechanism by simultaneously strengthening cellular antioxidant defenses and maintaining mitochondrial quantity and function.

In addition to enhancing thermotolerance through the regulation of DAF-16 and HSF-1, ALA further improves heat resistance by modulating mitochondrial dynamics and autophagy. Remarkably, although ALA does not influence the overall mitochondrial content following heat stress, it induces mitochondrial fragmentation and mitophagy—processes critical for improved heat resistance. Our data imply that ALA heightens heat resistance by facilitating these mitochondrial processes rather than amplifying mitochondrial numbers. Adaptation to heat stress often necessitates a quick adjustment in both the quantity and morphology of mitochondria to meet the new energy needs and metabolic state of the cell.[18,19] Mitochondrial fission plays a pivotal role in this process by increasing the number and surface area of the mitochondria, thereby enhancing the cell's ability to adapt to heat stress.[20] This process is intimately tied to mitophagy, wherein damaged mitochondrial fragments are sequestered and removed, optimizing mitochondrial function as a whole. By regulating mitochondrial quality through mitophagy, cellular energy metabolism stability is maintained, a process essential for effectively managing heat stress.[49]

ALA promotes the induction of autophagy, a cellular process that effectively addresses protein misfolding and organelle dysfunction caused by heat stress. The role of HLH-30 in autophagy is particularly significant, as its nuclear translocation and the expression of related genes enhance autophagic activity.[34,46] Our findings demonstrate that ALA facilitates the nuclear translocation of HLH-30 and upregulates the expression of autophagy-related genes, thereby enhancing autophagic activity and improving heat stress resistance.

Research across different model organisms has shown that inhibiting critical genes in the insulin-like signaling pathway can greatly enhance thermotolerance.[21–23] This effect is partly due to the activation of downstream transcription factors, especially the FOXO family, which are key regulators of numerous stress response genes.[50] Moreover, insulin-like signaling significantly influences protein homeostasis and antioxidant mechanisms, collectively supporting cellular survival during thermal stress.[51,52] In *C. elegans*, various cell types, including neurons, produce and secrete insulin-like peptides. Certain neurons release these peptides, potentially playing a central role in controlling metabolism, development, longevity, and stress responses *via* the gut–brain axis.[24] Our study reveals that ALA orchestrates inter-tissue stress responses by regulating neurotransmitter release and activating INS-19, an insulin-like peptide. As an insulin-like peptide, INS-19 is likely involved in the insulin/IGF-1 signaling pathway.[21,53] However, these proposed mechanisms remain speculative and require further experimental validation.

Transcriptional analysis indicates that ALA promotes the expression of INS-19, which subsequently influences the activity of HLH-30 and HSF-1, two key transcription factors involved in stress responses. Based on current findings, we propose that INS-19 may modulate HLH-30 and HSF-1 through multiple mechanisms. First, INS-19 may influence HLH-30 by altering its subcellular localization. Specifically, INS-19 could modulate the interaction between HLH-30 and proteins such as importin IMB-2 and the 14-3-3 protein, which are known to regulate HLH-30's nuclear translocation and activity.[46] This would enable HLH-30 to activate downstream genes involved in autophagy and lysosomal biogenesis, thereby enhancing cellular stress resilience. Additionally, INS-19 might directly or indirectly affect the expression of HLH-30 target genes, further amplifying its role in stress responses. Second, INS-19 activation could enhance HSF-1 activity by promoting its trimerization and nuclear translocation, a critical step for HSF-1 to function as a transcription factor. This would lead to the upregulation of heat shock proteins (HSPs), which improve protein folding and protect cells from thermal stress. INS-19 might also modulate post-translational modifications of HSF-1, such as phosphorylation or acetylation, which are known to regulate its transcriptional activity. INS-19 may facilitate cross-talk between HLH-30 and HSF-1, as both transcription factors are known to coordinate stress responses. For example, HLH-30-induced autophagy could support HSF-1-mediated protein homeostasis by clearing damaged proteins, while HSF-1-driven HSP expression might stabilize HLH-30 or its downstream effectors. While these mechanisms are supported by our transcriptional data and existing literature, they remain speculative and require further experimental validation. Future studies will focus on elucidating the precise molecular interactions between INS-19, HLH-30, and HSF-1, as well as their roles in heat resistance.

ALA is a naturally occurring compound present in foods like red meat, spinach, and broccoli, and is essential for stabilizing proteins and enzymes. Although we can synthesize ALA endogenously, this ability diminishes with age, underscoring ALA's important role in slowing aging and the potential benefits of supplementation. ALA uniquely regulates mitochondrial dynamics and induces autophagy and mitophagy through the transcription factor HLH-30/TFEB, thereby clearing damaged

mitochondria and reducing oxidative stress induced by thermal stress. This mechanism distinguishes ALA from many other antioxidants that primarily focus on scavenging reactive oxygen species (ROS). ALA activates the heat shock response (HSR) by upregulating heat shock factor 1 (HSF-1) and heat shock proteins (HSPs). This enhances protein folding and protects cells from thermal damage, similar to the action of other antioxidants.[54,55] At the same time, ALA regulates the expression of INS-19, an insulin-like peptide, which subsequently activates HLH-30 and HSF-1. This pathway further enhances cellular heat resistance by coordinating stress responses across tissues. This pathway differs from other known antioxidant mechanisms and highlights the multifaceted nature of ALA's action.

ALA enhanced organismal adaptability, promoting survival in heat stress. However, several critical questions remain unanswered. Specifically, the receptors for ALA and the neuronal populations responsible for INS-19 secretion need to be identified. Additionally, the mechanisms by which INS-19 interacts with the gut–brain axis to modulate HLH-30 and HSF-1 activity require further investigation. Understanding these interactions will provide deeper insights into how organisms maintain homeostasis and enhance thermal tolerance in response to environmental stressors.

5 Conclusions

ALA is a potent antioxidant that mitigates the adverse effects of heat stress across various biological systems. In this study, we demonstrate that ALA directly enhances heat resistance in *C. elegans*. Specifically, ALA upregulates heat shock proteins (HSPs) through heat shock factor 1 (HSF-1) and promotes mitochondrial fission and autophagy through the transcription factor HLH-30/TFEB. These processes preserve mitochondrial integrity and maintain cellular protein homeostasis. Notably, ALA activates HLH-30 and HSF-1 through the insulin-like peptide INS-19 to enhance heat resistance.

Collectively, these findings demonstrate that ALA mitigates heat stress through multiple mechanisms, including the upregulation of heat shock proteins and the enhancement of autophagy and mitophagy. Together, these processes work synergistically to alleviate heat stress-induced damage and enhance stress resistance in biological systems.

Given its multifaceted role in stress resistance, ALA has significant potential as a dietary supplement for enhancing heat stress tolerance. Future studies should explore its effects in other organisms and under different stress conditions to evaluate its broader applicability in food nutrition and dietary supplementation.

Author contributions

S. Z. and L. Z. conceived the project. L. Y. performed the experiments. L. Y. and Z. H. analyzed the data. L. Y, S. Z. and L. Z. wrote the manuscript with input from all authors.

Data availability

We have uploaded files named as S1 Data that contain all the observations that are reported as summary data in main figures. Each figure legend now includes callouts pointing to the raw data.

Conflicts of interest

The authors declare that they have no conflicts of interest with the contents of this article.

Acknowledgements

Some of the nematode strains used in this work were provided by the Caenorhabditis Genetics Center (University of Minnesota), which is supported by the NIH – Office of Research Infrastructure Programs (P40 OD010440). This work was supported by the National Natural Science Foundation of China (NSFC) grants (32470877 and 82401817).

References

1 K. Liu, E. Liu, L. Lin, Y. Hu, Y. Yuan and W. Xiao, L-Theanine mediates the p38MAPK signaling pathway to alleviate heat-induced oxidative stress and inflammation in mice, *Food Funct.*, 2022, **13**, 2120–2130.
2 L. Lin, S. Han, Z. Gong, F. Ding, Z. Liu and W. Xiao, L-theanine attenuates heat stress-induced proteotoxicity and alterations in carbohydrate and lipid metabolism via heat shock factor 1, *Food Funct.*, 2023, **14**, 6172–6186.
3 B. Wang, S. Liu, L. Lin, W. Xu, Z. Gong and W. Xiao, The protective effect of l-theanine on the intestinal barrier in heat-stressed organisms, *Food Funct.*, 2024, **15**, 3036–3049.
4 D. Yang, K. Xu, W. Wang, P. Chen, C. Liu, S. Liu, W. Xu and W. Xiao, Protective effects of l-theanine and dihydromyricetin on reproductive function in male mice under heat stress, *Food Funct.*, 2024, **15**, 7093–7107.
5 D. Kültz, Molecular and evolutionary basis of the cellular stress response, *Annu. Rev. Physiol.*, 2005, **67**, 225–257.
6 X. Chen, W. Liu, H. Li, J. Zhang, C. Hu and X. Liu, The adverse effect of heat stress and potential nutritional interventions, *Food Funct.*, 2022, **13**, 9195–9207.
7 A. Lavatelli, D. De Mendoza and M. C. Mansilla, Defining Caenorhabditis elegans as a model system to investigate lipoic acid metabolism, *J. Biol. Chem.*, 2020, **295**, 14973–14986.
8 J. Ye, H. Fan, R. Shi, G. Song, X. Wu, D. Wang, B. Xia, Z. Zhao, B. Zhao and X. Liu, Dietary lipoic acid alleviates autism-like behavior induced by acrylamide in adolescent mice: the potential involvement of the gut–brain axis, *Food Funct.*, 2024, **15**, 3395–3410.
9 P. Jiang, Z. Zhai, L. Zhao, K. Zhang and L. Duan, α–Lipoic acid alleviates dextran sulfate sodium salt–induced ulcera-

tive colitis via modulating the Keap1–Nrf2 signaling pathway and inhibiting ferroptosis, *J. Sci. Food Agric.*, 2024, **104**, 1679–1690.

10 S. Gonidakis, S. E. Finkel and V. D. Longo, Genome–wide screen identifies Escherichia coli TCA–cycle–related mutants with extended chronological lifespan dependent on acetate metabolism and the hypoxia–inducible transcription factor ArcA, *Aging Cell*, 2010, **9**, 868–881.

11 T. Kaletta and M. O. Hengartner, Finding function in novel targets: C. elegans as a model organism, *Nat. Rev. Drug Discovery*, 2006, **5**, 387–399.

12 E. L. Sonnhammer and R. Durbin, Analysis of protein domain families inCaenorhabditis elegans, *Genomics*, 1997, **46**, 200–216.

13 B. Song, H. Wang, W. Xia, B. Zheng, T. Li and R. H. Liu, Combination of apple peel and blueberry extracts synergistically induced lifespan extension via DAF-16 in Caenorhabditis elegans, *Food Funct.*, 2020, **11**, 6170–6185.

14 S. Kassis, M. Grondin and D. A. Averill-Bates, Heat shock increases levels of reactive oxygen species, autophagy and apoptosis, *Biochim. Biophys. Acta, Mol. Cell Res.*, 2021, **1868**, 118924.

15 D. Gagnon, H. Barry, A. Barhdadi, E. Oussaid, I. Mongrain, L.-P. Lemieux Perreault and M.-P. Dubé, A dataset of proteomic changes during human heat stress and heat acclimation, *Sci. Data*, 2023, **10**, 877.

16 C. Kumsta, J. T. Chang, J. Schmalz and M. Hansen, Hormetic heat stress and HSF-1 induce autophagy to improve survival and proteostasis in C. elegans, *Nat. Commun.*, 2017, **8**, 14337.

17 R. I. Morimoto, in *Cold Spring Harbor symposia on quantitative biology*, Cold Spring Harbor Laboratory Press, 2011, vol. 76, pp. 91–99.

18 A. M. Labrousse, M. D. Zappaterra, D. A. Rube and A. M. van der Bliek, C. elegans dynamin-related protein DRP-1 controls severing of the mitochondrial outer membrane, *Mol. Cell*, 1999, **4**, 815–826.

19 I. Manoli, S. Alesci, M. R. Blackman, Y. A. Su, O. M. Rennert and G. P. Chrousos, Mitochondria as key components of the stress response, *Trends Endocrinol. Metab.*, 2007, **18**, 190–198.

20 K. Palikaras, E. Lionaki and N. Tavernarakis, Coordination of mitophagy and mitochondrial biogenesis during ageing in C. elegans, *Nature*, 2015, **521**, 525–528.

21 G. McColl, A. N. Rogers, S. Alavez, A. E. Hubbard, S. Melov, C. D. Link, A. I. Bush, P. Kapahi and G. J. Lithgow, Insulin-like signaling determines survival during stress via post-transcriptional mechanisms in C. elegans, *Cell Metab.*, 2010, **12**, 260–272.

22 A. Taguchi and M. F. White, Insulin-like signaling, nutrient homeostasis, and life span, *Annu. Rev. Physiol.*, 2008, **70**, 191–212.

23 T. A. Rodrigues, J. Ispada, P. H. Risolia, M. T. Rodrigues, R. S. Lima, M. E. Assumpção, J. A. Visintin and F. F. Paula-Lopes, Thermoprotective effect of insulin-like growth factor 1 on in vitro matured bovine oocyte exposed to heat shock, *Theriogenology*, 2016, **86**, 2028–2039.

24 C. T. Murphy and P. J. Hu, Insulin/insulin-like growth factor signaling in C. elegans, in *WormBook: The Online Review of C. elegans Biology*, 2018.

25 L. A. Herndon, P. J. Schmeissner, J. M. Dudaronek, P. A. Brown, K. M. Listner, Y. Sakano, M. C. Paupard, D. H. Hall and M. Driscoll, Stochastic and genetic factors influence tissue-specific decline in ageing C. elegans, *Nature*, 2002, **419**, 808–814.

26 S. Chen, Y. Zhou, Y. Chen and J. Gu, fastp: an ultra-fast all-in-one FASTQ preprocessor, *Bioinformatics*, 2018, **34**, i884–i890.

27 D. Kim, B. Langmead and S. L. Salzberg, HISAT: a fast spliced aligner with low memory requirements, *Nat. Methods*, 2015, **12**, 357–360.

28 T. S. Tanabe, M. Grosser, L. Hahn, C. Kümpel, H. Hartenfels, E. Vtulkin, W. Flegler and C. Dahl, Identification of a novel lipoic acid biosynthesis pathway reveals the complex evolution of lipoate assembly in prokaryotes, *PLoS Biol.*, 2023, **21**, e3002177.

29 S. L. Rea, D. Wu, J. R. Cypser, J. W. Vaupel and T. E. Johnson, A stress-sensitive reporter predicts longevity in isogenic populations of Caenorhabditis elegans, *Nat. Genet.*, 2005, **37**, 894–898.

30 A. Olsen, M. C. Vantipalli and G. J. Lithgow, Lifespan extension of Caenorhabditis elegans following repeated mild hormetic heat treatments, *Biogerontology*, 2006, **7**, 221–230.

31 D. GuhaThakurta, L. Palomar, G. D. Stormo, P. Tedesco, T. E. Johnson, D. W. Walker, G. Lithgow, S. Kim and C. D. Link, Identification of a novel cis-regulatory element involved in the heat shock response in Caenorhabditis elegans using microarray gene expression and computational methods, *Genome Res.*, 2002, **12**, 701–712.

32 R. Higuchi-Sanabria, P. A. Frankino, J. W. Paul, S. U. Tronnes and A. Dillin, A futile battle? Protein quality control and the stress of aging, *Dev. Cell*, 2018, **44**, 139–163.

33 C. Kumsta and M. Hansen, Hormetic heat shock and HSF-1 overexpression improve C. elegans survival and proteostasis by inducing autophagy, *Autophagy*, 2017, **13**, 1076–1077.

34 X.-X. Lin, I. Sen, G. E. Janssens, X. Zhou, B. R. Fonslow, D. Edgar, N. Stroustrup, P. Swoboda and J. R. Yates, 3rd and G. Ruvkun, DAF-16/FOXO and HLH-30/TFEB function as combinatorial transcription factors to promote stress resistance and longevity, *Nat. Commun.*, 2018, **9**, 4400.

35 K. A. Wani, D. Goswamy, S. Taubert, R. Ratnappan, A. Ghazi and J. E. Irazoqui, NHR-49/PPAR-α and HLH-30/TFEB cooperate for C. elegans host defense via a flavin-containing monooxygenase, *eLife*, 2021, **10**, e62775.

36 M. Chamoli, A. Rane, A. Foulger, S. J. Chinta, A. A. Shahmirzadi, C. Kumsta, D. K. Nambiar, D. Hall, A. Holcom and S. Angeli, A drug-like molecule engages nuclear hormone receptor DAF-12/FXR to regulate mitophagy and extend lifespan, *Nat. Aging*, 2023, **3**, 1529–1543.

37 L. R. Lapierre, C. D. De Magalhaes Filho, P. R. McQuary, C.-C. Chu, O. Visvikis, J. T. Chang, S. Gelino, B. Ong, A. E. Davis and J. E. Irazoqui, The TFEB orthologue HLH-30 regulates autophagy and modulates longevity in Caenorhabditis elegans, *Nat. Commun.*, 2013, **4**, 2267.
38 A. Akbarian, J. Michiels, J. Degroote, M. Majdeddin, A. Golian and S. De Smet, Association between heat stress and oxidative stress in poultry; mitochondrial dysfunction and dietary interventions with phytochemicals, *J. Anim. Sci. Biotechnol.*, 2016, **7**, 1–14.
39 M. Rodriguez, L. B. Snoek, M. De Bono and J. E. Kammenga, Worms under stress: C. elegans stress response and its relevance to complex human disease and aging, *Trends Genet.*, 2013, **29**, 367–374.
40 S. Sarasija and K. R. Norman, A γ-secretase independent role for presenilin in calcium homeostasis impacts mitochondrial function and morphology in Caenorhabditis elegans, *Genetics*, 2015, **201**, 1453–1466.
41 J. E. Richmond, W. S. Davis and E. M. Jorgensen, UNC-13 is required for synaptic vesicle fusion in C. elegans, *Nat. Neurosci.*, 1999, **2**, 959–964.
42 S. Speese, M. Petrie, K. Schuske, M. Ailion, K. Ann, K. Iwasaki, E. M. Jorgensen and T. F. Martin, UNC-31 (CAPS) is required for dense-core vesicle but not synaptic vesicle exocytosis in Caenorhabditis elegans, *J. Neurosci.*, 2007, **27**, 6150–6162.
43 V. Prahlad and R. I. Morimoto, Integrating the stress response: lessons for neurodegenerative diseases from C. elegans, *Trends Cell Biol.*, 2009, **19**, 52–61.
44 M. Costa-Mattioli and P. Walter, The integrated stress response: From mechanism to disease, *Science*, 2020, **368**, eaat5314.
45 S.-H. Lee, M.-H. Sun, W.-J. Jiang, X.-H. Li, G. Heo, D. Zhou, Z. Chen and X.-S. Cui, Alpha-lipoic acid attenuates heat stress-induced apoptosis via upregulating the heat shock response in porcine parthenotes, *Sci. Rep.*, 2023, **13**, 8427.
46 H. Colino-Lage, D. Guerrero-Gómez, E. Gómez-Orte, X. González, J. A. Martina, T. B. Dansen, C. Ayuso, P. Askjaer, R. Puertollano and J. E. Irazoqui, Regulation of Caenorhabditis elegans HLH-30 subcellular localization dynamics: Evidence for a redox-dependent mechanism, *Free Radicals Biol. Med.*, 2024, **223**, 369–383.
47 M. J. Rodriguez-Colman, T. B. Dansen and B. M. Burgering, FOXO transcription factors as mediators of stress adaptation, *Nat. Rev. Mol. Cell Biol.*, 2024, **25**, 46–64.
48 C. Konwar, J. Maini and D. Saluja, Understanding Longevity: SIN-3 and DAF-16 Revealed as Independent Players in Lifespan Regulation, *J. Gerontol., Ser. A*, 2024, glae160.
49 Y. Chen, R. Leboutet, C. Largeau, S. Zentout, C. Lefebvre, A. Delahodde, E. Culetto and R. Legouis, Autophagy facilitates mitochondrial rebuilding after acute heat stress via a DRP-1–dependent process, *J. Cell Biol.*, 2021, **220**, e201909139.
50 N. E. Gruntenko, N. V. Adonyeva, E. V. Burdina, E. K. Karpova, O. V. Andreenkova, D. V. Gladkikh, Y. Y. Ilinsky and I. Y. Rauschenbach, The impact of FOXO on dopamine and octopamine metabolism in Drosophila under normal and heat stress conditions, *Biol. Open*, 2016, **5**, 1706–1711.
51 C. Lennicke and H. M. Cochemé, Redox regulation of the insulin signalling pathway, *Redox Biol.*, 2021, **42**, 101964.
52 R. S. Lima, P. H. Risolia, J. Ispada, M. E. Assumpção, J. A. Visintin, C. Orlandi and F. F. Paula-Lopes, Role of insulin-like growth factor 1 on cross-bred Bos indicus cattle germinal vesicle oocytes exposed to heat shock, *Reprod., Fertil. Dev.*, 2017, **29**, 1405–1414.
53 A. D. Ritter, Y. Shen, J. F. Bass, S. Jeyaraj, B. Deplancke, A. Mukhopadhyay, J. Xu, M. Driscoll, H. A. Tissenbaum and A. J. Walhout, Complex expression dynamics and robustness in C. elegans insulin networks, *Genome Res.*, 2013, **23**, 954–965.
54 F. Xu, R. Li, E. D. Von Gromoff, F. Drepper, B. Knapp, B. Warscheid, R. Baumeister and W. Qi, Reprogramming of the transcriptome after heat stress mediates heat hormesis in Caenorhabditis elegans, *Nat. Commun.*, 2023, **14**, 4176.
55 W. I. Jiang, H. De Belly, B. Wang, A. Wong, M. Kim, F. Oh, J. DeGeorge, X. Huang, S. Guang and O. D. Weiner, Early-life stress triggers long-lasting organismal resilience and longevity via tetraspanin, *Sci. Adv.*, 2024, **10**, eadj3880.